



Published in final edited form as:

Drug Metab Lett. 2012 ; 6(4): 275–284.

Development of Flavone Propargyl Ethers as Potent and Selective Inhibitors of Cytochrome P450 Enzymes 1A1 and 1A2

Jayalakshmi Sridhar^{1,*}, Jamie Ellis¹, Patrick Dupart¹, Jiawang Liu¹, Cheryl L. Stevens², and Maryam Foroozesh¹

¹Department of Chemistry, Xavier University of Louisiana, 1 Drexel Dr., New Orleans, LA 70125, USA

²Ogden College of Science and Engineering, Western Kentucky University, 1906 College Heights Boulevard #11075, Bowling Green, Kentucky 42101-1075, USA

Abstract

Naturally occurring flavonoids are known to be metabolized by several cytochrome P450 enzymes including P450s 1A1, 1A2, 1B1, 2C9, 3A4, and 3A5. In general flavonoids can act as substrates, inducers, and/or inhibitors of P450 enzymes. The position of the substituents on the flavone backbone has been shown to impact the biological activity against P450 enzymes. To explore the effect of a propargyl ether substitution on flavones and flavanones, 2'-flavone propargyl ether (2'-PF), 3'-flavone propargyl ether (3'-PF), 4'-flavone propargyl ether (4'-PF), 5-flavone propargyl ether (5-PF), 6-flavone propargyl ether (6-PF), 7-flavone propargyl ether (7-PF), 6-flavanone propargyl ether (6-PFN), and 7-flavanone propargyl ether (7-PFN) were synthesized. All of the newly synthesized compounds and the parent hydroxy flavones were tested for both direct inhibition and mechanism-based inhibition of cytochrome P450 enzymes 1A1, 1A2, 2A6, and 2B1. The flavone propargyl ether derivatives were found to be more potent inhibitors of P450s 1A1 and 1A2. None of the flavones and flavanones in our study showed any inhibition of P450 2A6. Only 2'-PF and 6-PFN inhibited P450 2B1. 3'-PF showed direct inhibition of P450 1A1 with the highest observed potency of 0.02 μM , in addition to its ability to cause mechanism-based inhibition with K_I and $k_{inactivation}$ values of 0.24 μM and 0.09 min^{-1} for this enzyme. 7-Hydroxy flavone also exhibited mechanism-based inhibition of P450 1A1 with K_I and $k_{inactivation}$ values of 2.43 μM and 0.115 min^{-1} . Docking studies and QSAR studies on P450 enzymes 1A1 and 1A2 were performed which revealed important insights into the nature of binding of these molecules and provided us with good QSAR models that can be used to design new flavone derivatives.

Keywords

Cytochrome P450 enzyme; flavone propargyl ethers; mechanism based inhibition; QSAR models

©2012 Bentham Science Publishers

*Address correspondence to this author at the Department of Chemistry, Xavier University of Louisiana, 1 Drexel Dr., New Orleans, LA 70125, USA; Tel: 504-520-7519; Fax: 504-520-7942; jsridhar@xula.edu.

CONFLICT OF INTEREST

The author(s) confirm that this article content has no conflict of interest.

INTRODUCTION

Flavonoids are phytochemicals that are widely found in fruits and vegetables and are important constituents of the human diet [1]. These important biologically and pharmacologically active compounds have been shown to act as antioxidant, anti-inflammatory, antimutagenic, antimicrobial, anti-allergic, and drug-metabolizing enzyme inducing agents, thereby preventing cancer, cardiovascular, and other diseases [2-8]. Flavones and flavonols are the major components of naturally occurring flavonoids. The biological activities of hydroxy and methoxy flavones towards P450 enzymes have been shown to be influenced by the position of the functional groups on the flavone backbone [9-12]. Structural modifications of flavonoids that impact their biological activities have been studied by many laboratories [9, 13-15]. Flavonoids belonging to several well-defined classes are known to induce or inhibit cytochrome P450s 1A1, 1A2, 1B1, 2C9, 3A4, and 3A5 [9, 13, 16-23] and thereby alter the response of these enzymes to other xenobiotic or endogenous compounds.

Polyaromatic hydrocarbons (PAHs) have been shown to cause two types of inhibition of P450 enzymes, direct inhibition and mechanism-based inhibition (suicide inhibition). For the mechanism-based inhibition process, three pathways have been observed. The first pathway involves oxidation of the inhibitor to a product that reacts with the protein to form N-alkylation of the iron porphyrin [24-26]; the second pathway entails the inhibitor covalently modifying the apoprotein [27, 28]; and the third pathway involves the heme-product adduct to irreversibly bind to the protein [29-31]. Allenic and acetylenic compounds often exhibit the first pathway of mechanism-based inhibition. We have earlier shown that aryl acetylenes containing a terminal alkyne group function as suicide inhibitors of cytochrome P450 1A and 2B enzymes [32-37]. The triple bond of the terminal acetylene is oxidized by the P450 enzyme to form a reactive ketene intermediate by 1,2-hydrogen shift. The ketene intermediate can then react with the heme nitrogen resulting in a time-dependent destruction of the heme [24-26], or covalently bond with a nucleophilic residue of the protein thereby inactivating the enzyme [38, 39]. Propargyl derivatives of adamantanes and naphthoflavones have shown increased inhibition potency and selectivity for cytochrome P450 enzymes [13, 36]. To explore the effect of a propargyl group substitution on flavones, 2'-flavone propargyl ether (2'-PF), 3'-flavone propargyl ether (3'-PF), 4'-flavone propargyl ether (4'-PF), 5-flavone propargyl ether (5-PF), 6-flavone propargyl ether (6-PF), and 7-flavone propargyl ether (7-PF) were synthesized. Flavanones have been shown to be metabolized to flavones, flavonol, and isoflavones by cytochrome P450 enzymes [40]. To explore their potential as inhibitors, propargyl ether substituents were incorporated to obtain 6-flavanone propargyl ether (6-PFN) and 7-flavanone propargyl ether (7-PFN). All of the synthesized compounds and the parent hydroxy flavones were tested for both direct inhibition and mechanism-based inhibition against cytochrome P450 enzymes 1A1, 1A2, 2A6, and 2B1.

MATERIALS AND METHODS

Chemistry

The starting materials for the synthesis of the flavone propargyl ethers were purchased from INDOFINE Chemical Company, Inc. RP-HPLC was performed on a Hewlett Packard Series 1050 (Column: phenomenex Gemini-NX 5 μ m C18 110A). Mass spectral data were determined by Agilent 6890 GC with a 5973 MS. ^1H NMR and ^{13}C NMR spectra were recorded on Varian 300 MHz and Varian 400 MHz NMR spectrometers. Elemental analysis was performed by Atlantic Microlab, Inc. (Norcross, GA).

The hydroxy flavone starting material was dissolved in 40 mL of dry dimethyl sulfoxide (DMSO) under nitrogen atmosphere, followed by the slow addition of sodium hydride (1.1 eq., 1.9 mM, 76 mg of 60% dispersion in mineral oil (Aldrich Chemical Co.)). Propargyl bromide (2 eq., 3.56 mM, 0.4 mL of 80% solution in toluene, (Aldrich Chemical Co.)) was then added and the reaction mixture was left to stir under nitrogen atmosphere to room temperature for 24 h. An equal volume of water was then added, and the mixture was left to stir for an additional 12 h. The resulting precipitate was filtered and washed with water, dried and purified by silica gel flash column chromatography using 1% methanol in chloroform as the solvent. The fractions containing the fluorescent product were combined, the solvent evaporated, and the solid recrystallized from ethanol/water. The yield of recrystallized product ranged from 40% to 60% for the eight target compounds.

2'-Flavone Propargyl Ether—M.P. = 118-119.5 °C. ^1H NMR (400 MHz, CDCl_3) δ 2.54 (t, J = 2.4 Hz, 1H), 4.81 (d, J = 2.4 Hz, 2H), 7.07 (s, 1H), 7.12-7.20 (m, 2H), 7.38 (dt, J = 7.2 Hz, 0.8 Hz, 1H), 7.45-7.54 (m, 2H), 7.65 (dt, J = 7.2 Hz, 2.0 Hz, 1H), 7.86 (dd, J = 7.6 Hz, 1.6 Hz, 1H), 8.21 (dd, J = 8.0 Hz, 1.6 Hz, 1H). ^{13}C NMR (300 MHz, CDCl_3) δ 56.55, 76.60, 78.05, 113.06, 113.76, 118.25, 121.93, 122.05, 124.07, 125.13, 125.84, 129.78, 132.37, 133.75, 155.98, 156.74, 160.99, 178.89. Anal. ($\text{C}_{18}\text{H}_{12}\text{O}_3$) C, H, O. Calc. C = 78.25%, H = 4.38%, O = 17.37%; Found C = 77.26%, H = 4.54%, O = 17.57%

3'-Flavone Propargyl Ether—M.P. = 133.5-135.0 °C. ^1H NMR (400 MHz, CDCl_3) δ 2.57 (s, 1H), 4.80 (s, 2H), 6.85 (s, 1H), 7.12 (m, 1H), 7.37-7.61 (m, 5H), 7.68-7.74 (m, 1H), 8.25 (d, J = 8.0 Hz, 1H). ^{13}C NMR (300 MHz, CDCl_3) δ 56.32, 76.31, 108.12, 113.27, 118.30, 118.39, 119.86, 125.52, 125.38, 130.38, 134.06, 156.26, 157.08, 158.26, 163.33, 178.71. Anal. ($\text{C}_{18}\text{H}_{12}\text{O}_3$) C, H, O; Calc. C = 78.25%, H = 4.38%, O = 17.37%; Found C = 77.02%, H = 4.35%, O = 17.98%

4'-Flavone Propargyl Ether—M.P. = 165-166.5 °C. ^1H NMR (400 MHz, CDCl_3) δ 2.57 (s, 1H), 4.80 (s, 2H), 6.78 (s, 1H), 7.12 (d, J = 8.89 Hz, 1H), 7.42 (t, J = 7.41 Hz, 1H), 7.56 (d, J = 7.41 Hz, 1H), 7.73 (dt, J = 8.89 Hz, 1.48 Hz, 1H), 7.92 (d, J = 8.89 Hz, 1H), 8.24 (dd, J = 8.89, 1.48 Hz, 1H). ^{13}C NMR (300 MHz, CDCl_3) δ 56.18, 76.36, 78.05, 106.77, 115.65, 118.16, 124.25, 125.33, 125.96, 128.20, 133.78, 156.47, 160.49, 163.42, 178.51. Anal. ($\text{C}_{18}\text{H}_{12}\text{O}_3$) C, H, O. Calc. C = 78.25%, H = 4.38%, O = 17.37%; Found C = 78.29%, H = 4.31%, O = 17.45%

5-Flavone Propargyl Ether—M.P. = 139.5-140.5 °C. ¹HNMR (400 MHz, CDCl₃) δ2.54 (t, *J* = 2.4 Hz, 1H), 4.90 (d, *J* = 2.4 Hz, 2H), 6.71 (s, 1H), 7.01 (d, *J* = 8.4 Hz, 1H), 7.187 (d, *J* = 8.4 Hz, 1H), 7.47-7.51 (m, 3H), 7.57 (t, *J* = 8.4 Hz, 1H), 7.85-7.88 (m, 2H). ¹³CNMR (300 MHz, CDCl₃) δ57.64, 76.59, 78.36, 109.28, 110.13, 111.75, 126.30, 129.18, 131.60, 133.62, 157.59, 158.47, 161.42, 178.03. Anal. (C₁₈H₁₂O₃) C, H, O. Calc. C = 78.25%, H = 4.38%; Found C = 77.75%, H = 4.27%

6-Flavone Propargyl Ether—M.P. = 135.0-136.0 °C. ¹HNMR (400 MHz, CDCl₃) δ2.56 (t, *J* = 2.0 Hz, 1H), 4.76 (d, *J* = 2.0 Hz, 2H), 6.78 (s, 1H), 7.31 (dd, *J* = 2.8 Hz, 8.8 Hz, 1H), 7.44-7.54 (m, 4H), 7.65 (d, *J* = 3.2 Hz, 1H), 7.84-7.91 (m, 2H). ¹³CNMR (300 MHz, CDCl₃) δ56.65, 76.30, 78.08, 107.11, 119.86, 124.26, 124.75, 126.44, 129.23, 131.72, 132.01, 151.65, 155.06, 163.39, 178.18. Anal. (C₁₈H₁₂O₃) C, H, O. Calc. C = 78.25%, H = 4.38%, O = 17.37%; Found C = 78.17%, H = 4.49%, O = 17.48%

7-Flavone Propargyl Ether—M.P. = 194.0-196.0 °C. ¹HNMR (400 MHz, CDCl₃) δ2.61 (d, *J* = 2.4 Hz, 1H), 4.82 (d, *J* = 2.4 Hz, 2H), 6.77 (s, 1H), 7.04-7.09 (m, 2H), 7.51-7.58 (m, 3H), 7.90-7.94 (m, 2H), 8.16 (d, *J* = 9.2 Hz, 1H). ¹³CNMR (300 MHz, CDCl₃) δ56.70, 76.27, 78.03, 107.02, 107.15, 119.89, 124.4, 126.53, 129.26, 131.78, 132.08, 151.78, 155.13, 176.30. Anal. (C₁₈H₁₂O₃) C, H, O. Calc. C = 78.25%, H = 4.38%, O = 17.37%; Found C = 78.25%, H = 4.22%, O = 17.41%

6-Flavonone Propargyl Ether—M.P. = 99.5-100.0 °C. ¹HNMR (400 MHz, CDCl₃) δ2.54 (t, *J* = 2 Hz, 1H), 2.88, (dd, *J* = 2 Hz, 16.9 Hz, 1H), 3.08, (dd, *J* = 16.8 Hz, 15.6 Hz, 1H), 4.70 (s, 2H), 5.45 (dd, *J* = 3.8 Hz, 13.4 Hz, 1H), 7.02 (d, *J* = 9.6 Hz, 1H), 7.18 (dd, *J* = 9.6 Hz, 3.8 Hz, 1H), 7.36-7.51 (m, 5H). ¹³CNMR (300 MHz, CDCl₃) δ44.90, 56.85, 76.13, 78.56, 80.08, 109.89, 119.91, 121.20, 126.13, 126.20, 126.34, 126.48, 129.11, 129.20, 139.14, 152.51, 157.17, 192.09. Anal. (C₁₈H₁₄O₃) C, H, O. Calc. C = 77.68%, H = 5.07%, O = 17.25%; Found C = 77.66%, H = 4.99%, O = 17.09%

7-Flavonone Propargyl Ether—M.P. = 58.0-59.0 °C. ¹HNMR (400 MHz, CDCl₃) δ2.56 (t, *J* = 2.4 Hz, 1H), 2.84 (dd, *J* = 17.2 Hz, 2.8 Hz, 1H), 3.05 (dd, *J* = 16.8 Hz, 13.2 Hz, 1H), 4.72 (d, *J* = 2.4 Hz, 2H), 5.48 (dd, *J* = 13.2 Hz, 2.8 Hz, 1H), 6.61 (d, *J* = 2.4 Hz, 1H), 6.68 (dd, *J* = 8.8 Hz, 2.4 Hz, 1H), 7.40-7.52 (m, 5H), 7.89 (d, *J* = 8.8 Hz, 1H). ¹³CNMR (300 MHz, CDCl₃) δ44.57, 56.26, 76.57, 77.42, 80.28, 102.46, 110.78, 115.81, 26.39, 129.05, 139.01, 164.20, 190.66. Anal. (C₁₈H₁₄O₃) C, H, O. Calc. C = 77.68%, H = 5.07%, O = 17.25%; Found C = 77.92%, H = 5.99%, O = 16.66%

ASSAYS

Rat P4502B1 supersomes (rat P4502B1 + P450 reductase + cytochrome b5), and human P450 1A1, 1A2, and 2A6 supersomes (human P450 enzymes + P450 reductase) were purchased from B.D. Biosciences Corporation (Woburn, MA, USA). All other chemicals were purchased from Sigma Aldrich Company (Milwaukee, WI).

The P450 1A1, 1A2, and 2B1-dependent activities were assayed in resorufin alkyl ether dealkylation assays using resorufin ethyl ether, resorufin methyl ether, and resorufin pentyl

ether fluorescent substrates respectively [41]. P450 2A6 dependent 7-hydroxylation of coumarin was used in a similar assay with minor differences as described below for measuring P450 2A6 activity [42, 43].

ETHOXYRESORUFIN O-DEETHYLATION (EROD), METHOXYRESORUFIN O-DEMETHYLATION (MROD), PENTOXYRESORUFIN O-DEPENTYLATION (PROD), AND COUMARIN 7-HYDROXYLATION ASSAYS

Potassium phosphate buffer (1760 μL of a 0.1 M solution, pH 7.6) was placed in a 1.0 cm quartz cuvette, and 10 μL of a 1.0 M MgCl_2 solution, 10 μL of a 1.0 mM corresponding resorufin or coumarin substrate solution (final concentration of 5 μM) in DMSO, 10 μL of the microsomal P450 protein (final concentration of 5 nM), and 10 μL of an inhibitor solution in DMSO were added. For the controls, 10 μL of pure DMSO was added in place of the inhibitor solution. The reaction was initiated by the addition of 200 μL of a NADPH regenerating solution. The regenerating solution was prepared by combining 797 μL of a 0.10 M potassium phosphate buffer solution (pH 7.6), 67 μL of a 15 mM NADP^+ solution in buffer, 67 μL of a 67.5 mM glucose-6-phosphate solution in buffer, and 67 μL of a 45 mM MgCl_2 solution, and incubating the mixture for 5 minutes at 37°C before the addition of 3 units of glucose 6-phosphate dehydrogenase/mL and a final 5 minute incubation at 37°C. The final assay volume was 2.0 mL. The production of resorufin anion was monitored by a spectrofluorimeter (OLIS DM 45 Spectrofluorimetry System) at 535 nm excitation and 585 nm emission, with a slit width of 2 nm. The production of 7-hydroxycoumarin was monitored at 338 nm excitation and 458 nm emission, with a slit width of 2 nm. The reactions were performed at 37°C. For each inhibitor, a number of assay runs were performed using varying inhibitor concentrations (ranging from 0.1 to 100 M). At least five concentrations of each inhibitor showing 20-80% inhibition were tested.

DATA ANALYSIS [33]

The data obtained from these assays were analyzed by a computer analysis method of the reaction progress curve in the presence of various inhibitor concentrations and in the absence of the inhibitor as the control run. Results are tabulated in Table 1. A second order curve describing product formation with respect to reaction time in seconds was obtained for each inhibitor concentration and the control. The Microsoft Excel Program was used to fit the data (Fluorescence intensity vs. Time) obtaining the parameters of the best-fit second order curves ($y=ax^2+bx+c$). Using the parameters (Coefficient b in the second order equation is enzymatic activity) obtained from the above, activities were calculated using first order derivatives. Dixon plots were used by plotting the reciprocals of enzymatic activity ($1/v$) vs. inhibitor concentrations [I] in order to determine IC_{50} values (x-intercepts) for the inhibitors.

PRE-INCUBATION ASSAYS IN THE PRESENCE AND ABSENCE OF NADPH

To confirm mechanism-based inhibition, pre-incubation assays were performed as follows. All assay solution components had the same concentrations as in the above assays. For pre-incubation assays in the presence of NADPH, potassium phosphate buffer (1560 μL of a 0.1

M solution, pH 7.6) was placed in a 1.0 cm quartz cuvette followed by 10 μL of a 1.0 M MgCl_2 solution, 10 μL of the microsomal P450 protein, 10 μL of an inhibitor solution in DMSO (for the control, 10 μL of pure DMSO was added in the place of the inhibitor solution), and 200 μL of a NADPH regenerating solution. The assay mixture was incubated for five minutes at 37°C before reaction initiation by the addition of 200 μL of buffer and 10 μL of the corresponding substrate solution. The final assay volume was 2.0 mL. The production of 7-hydroxyresorufin was monitored at 535 nm excitation and 585 nm emission. The production of 7-hydroxycoumarin was monitored at 338 nm excitation and 458 nm emission. The reactions were performed at 37°C. For each inhibitor, a number of assay runs were performed using varying inhibitor concentrations. For the pre-incubation assays in the absence of NADPH, potassium phosphate buffer (1760 μL of a 0.1 M solution, pH 7.6) was placed in a 1.0 cm quartz cuvette followed by 10 μL of a 1.0 M MgCl_2 solution, 10 μL of the microsomal P450 protein, and 10 μL of an inhibitor solution in DMSO (for the control, 10 μL of pure DMSO was added in the place of the inhibitor solution). The assay mixture was incubated for five minutes at 37°C before reaction initiation by the addition of 200 μL of the NADPH regenerating solution and 10 μL of the corresponding substrate solution. The final assay volume was 2.0 mL. The production of P450-dependent reaction products were monitored as previously described [32]. The reactions were performed at 37°C. For each inhibitor, a number of assay runs were performed using varying inhibitor concentrations.

MODELING STUDIES

All *in silico* studies were carried out using the Molecular Operating Environment (MOE) Program (Chemical Computing Group, Montreal, Canada). The coordinates of the template P450 enzymes 1A2 (PDB ID: 2HI4) and 2A6 (PDB ID: 1Z10) were taken from the Protein Data Bank (<http://www.rcsb.org>). Oxygen atoms representing water were removed and hydrogen atoms were added to the template proteins using Amber ff99 force field. The homology models of P450s 1A1 and 2B1 built for an earlier study were used for the present docking studies [44].

BINDING MODES BY DOCKING SIMULATION

The structures of the molecules used in this study are given in Fig. (1). The 3D structures of the molecules were built using the Tripos SYBYL 7.3 Program. Initial geometric optimizations of the ligands were carried out using the standard MMFF94 force field, with a 0.001 kcal mol⁻¹ energy gradient convergence criterion and a distance-dependent dielectric constant employing Gasteiger and Marsili charges. Additional geometric optimizations were performed using the semi-empirical method molecular orbital package (MOPAC). The compounds were docked into the binding pockets of P450 enzymes using two programs, MOE and FlexX (Tripos). The consensus binding postures of the inhibitors were obtained by visual inspection of the docking simulations and their docking scores. The docked complexes were then minimized in three steps using MOE Energy Minimize application. Amber ff99 was used for standard residues of the protein and partial charges were calculated as required for this force field. The non-standard force field parameters for heme and the cysteine-iron bond were taken from the literature [45]. MOE Energy minimization consists of finding a set of atomic coordinates that correspond to a local minimum of the molecular

energy function (we used the potential energy model) by applying large scale non-linear optimization techniques to calculate a conformation (near to the starting geometry) for which the forces on the atoms are zero [46]. MOE uses a success of three methods to effect an energy minimization: Steepest Descent (SD), Conjugate Gradient (SG) and Truncated Newton (TN) controlled by the root mean square (RMS) gradient of energy falling below 0.1 kcal A⁻¹. In addition, atoms may be fixed during the calculation. First, hydrogen atom positions were relaxed by holding other atoms fixed. This was followed by allowing all side chain atoms to relax while holding the backbone atoms fixed. Finally, the entire structure was relaxed until root mean square (RMS) gradient of energy was less than 0.1 kcal A⁻¹. Through all of the minimization steps, the planar structure of the heme residue was maintained.

3D QSAR WITH COMFA

The QSAR studies were performed on Red Hat Linux computers running the Tripos SYBYLX1.3 program. Initial geometric optimizations of the ligands were carried out using the standard MMFF94 force field, with a 0.001 kcal/mol energy gradient convergence criterion and a distance-dependent dielectric constant employing Gasteiger charges. The SYBYL automated alignment feature was utilized for aligning the databases. The QSAR Project Manager module of SYBYLX1.3 was used. The new QSAR Project Manager module streamlines the organization of QSAR datasets, QSAR models, and QSAR predictions thereby supporting combinatorial model creation. The aligned database was imported into the QSAR Project Manager and the training sets and test sets were created. Descriptors such as COMFA (Comparative Molecular Field Analysis; operates on steric and electrostatic energy values at points in space surrounding the molecules), ClogP, molecular weight, CPSA (Charged Partial Surface Area; combines molecular surface area and partial atomic charges), hydrogen bond acceptor and donor fields were used for generation of good QSAR models. The methoxy flavones and naphthoflavone propargyl ethers included in the dataset for QSAR studies are 3'-methoxy flavone (3'-FM), 3',4'-dimethoxy flavone (3',4'-DFM), 4'-methoxy flavone (4'-FM), α -naphthoflavone-2'-propargyl ether (2'- α PNF), β -naphthoflavone-2'-propargyl ether (2'- β PNF), α -naphthoflavone-4'-propargyl ether (4'- α PNF), and β -naphthoflavone-4'-propargyl ether (4'- β PNF) from our earlier publications [13, 47].

RESULTS AND DISCUSSION

A total of eight synthesized flavone propargyl ethers and flavanone propargyl ethers along with the parent hydroxy flavones (Fig. 1) were assayed at five effective concentrations as potential inhibitors of EROD, MROD, and PROD activities in human P450s 1A1 and 1A2 and rat P4502B1 supersomes (Table 1). The P450 2A6 inhibition activity of the compounds was assayed by using the P450 2A6-dependent 7-hydroxylation of coumarin using human P450 2A6 supersomes. Two types of inhibition (direct inhibition and mechanism-based inhibition) were evaluated for the compounds in the present study. A direct inhibitor is a straightforward competitive inhibitor of the enzyme. A mechanism-based inhibitor is one that is metabolized by the enzyme into a reactive intermediate that further reacts with the

enzyme to form a complex that is no longer enzymatically active. This method of inhibition is time and cofactor dependent.

The propargyl ether derivatives showed a 4-25 fold increase in inhibition potency when compared to the corresponding hydroxy flavones (Table 1). This clearly illustrated the veracity of introducing the acetylenic substituent group in the chemical scaffold while developing P450 inhibitors. Among the hydroxy flavones, 5-hydroxy flavone (5-HF) showed the best inhibition potency for the P450 enzyme 1A2 with an IC_{50} value of 0.31 μ M. All the flavone propargyl ethers showed low micromolar or submicromolar potency against the P450 enzymes 1A1 and 1A2. 3'-FLAVONE propargyl ether (3'-PF) showed excellent inhibition of P450 1A1 with an IC_{50} of 0.02 μ M. Both of the flavanone propargyl ethers (6-PFN and 7-PFN) inhibited P450 1A1 with IC_{50} values of 5.77 and 5.98 μ M respectively. Only 6-PFN did not show inhibition of P450 enzyme 1A2. Two compounds [2'-flavone propargyl ether (2'-PF) and 6-flavanone propargyl ether (6-PFN)] inhibited P450 2B1 enzyme with a potency in the low micromolar range (9.66 and 2.35 μ M respectively). None of the compounds studied inhibited P450 2A6.

3'-flavone propargyl ether (3'-PF) and 7-hydroxy flavone (7-HF) exhibited mechanism-based inhibition of P450 enzyme 1A1 (Table 2). Figs. (2A and 2B) depict the plots of the results of the NADPH-dependency assays of compounds 3'-PF and 7-HF for this enzyme. The NADPH-dependency assay allows affirmation of mechanism-based inhibition versus direct inhibition of the compound. For mechanism-based inhibition of P450 1A1 by the compounds 3'-PF and 7-HF, the rate constants for maximal inactivation at saturation ($k_{inactivation}$) were 0.09 and 0.115 min^{-1} respectively, and the concentrations required to produce one-half of the maximal rates of inactivation (K_I) were 0.24 and 2.43 μ M respectively.

P450s 1A1 and 1A2 have larger binding cavities with several phenylalanine residues capable of forming interactions with the bound ligands. The numbers of polar and hydrophobic residues in the binding cavities of these two enzymes are comparable. Our earlier studies on polyaromatic hydrocarbons (PAHs) have indicated the importance of aromatic interactions in determining the inhibition potency for P450 1A2 [44]. Docking studies of the compounds in this study on the P450 enzymes 1A1 and 1A2 revealed that all of the compounds indeed display multiple π - π interactions with the phenylalanine residues lining the catalytic pockets. For P450 1A2, 5-hydroxy flavone (5-HF) depicted a binding posture that was different from those of the other hydroxy flavones (Fig. 3A) in that the non-substituted phenyl group of 5-HF is oriented towards the heme residue, making it susceptible to oxidation by the enzyme, thereby increasing its potency. All of the other hydroxy flavones orient the hydroxyl functional group to the heme residue of P450 1A2 in the majority of the binding modes displayed during docking studies. The end to end distance of the flavone propargyl ethers is more than that of hydroxy flavones. This enables the propargyl groups to position their triple bonds closer to the catalytic center (ie. the heme residue) while still maintaining optimum π - π interactions with the phenylalanine residues. This would contribute to an increase in potency as evidenced by the IC_{50} values of flavone propargyl ethers for P450s 1A1 and 1A2. The docking posture of 3'-flavone propargyl ether (3'-FP, Fig. 3B) in the binding pocket of P450 1A1 showed that the terminal carbon of the

acetylenic group is at a distance of 5.26 Å from the heme-Fe atom in close proximity to the Arg106 residue. The oxidation of the triple bond could lead to the formation of the unstable ketene intermediate that could acylate the adjacent arginine residue (R106) or the heme residue in order to cause mechanism-based inhibition of P450 1A1.

To better understand the structural features responsible for the potency of the flavones, quantitative structure activity studies (QSAR) with COMFA were pursued using the SYBYLX1.3 software. Methoxy flavones and naphthoflavone propargyl ethers from our earlier studies [13, 47] that were found to be good inhibitors of P450s 1A1 and 1A2 were also included in the QSAR studies to obtain a robust set of compounds. The summary of the QSAR studies has been outlined in our review on the QSAR studies on multiple P450 enzymes [48]. The database of flavones studied with P450 enzymes 1A1 and 1A2 consisted of 21 and 19 compounds, respectively. Three compounds out of each database were chosen randomly for the test set. The QSAR analysis of the models for P450s 1A1 and 1A2 gave a cross-validated result of $q^2 = 0.653$ and 0.648 with five and two components, respectively. The conventional r^2 values were 0.982 and 0.893 with a standard error of 0.164 and 0.177 for the P450 1A1 and 1A2 models, respectively. The descriptors that contributed to the model for P450 1A1 are ClogP (17.7%), COMFA steric (32.7%), COMFA electrostatic (28.2%), molecular weight (15.3%), acceptor field (0.3%), and donor field (5.8%). The ClogP descriptor contributed more than half (54.1%) the coefficient for the P450 1A2 inhibitors QSAR model, with the other descriptors COMFA steric, COMFA electrostatic, and molecular weight contributing 12.2%, 19.0% and 14.6%, respectively. The log values of the actual and predicted inhibition are given in Tables **3A** and **3B** for the P450 1A1 and 1A2 models along with the graphical representation of the correlation between them (Figs. **4A** and **4B**). The QSAR 3D coefficient contour maps for the most active compounds of P450 1A1 (3'-PF) and 1A2 (5-HF) databases are shown in Figs. (**5A** and **5B**). Desirable and undesirable steric bulks are displayed in green and yellow contours, respectively. The electrostatic contributions for potency are shown as blue contour favoring positively charged substituents and red contour favoring negatively charged substituents. Fig. (**5**) clearly illustrates that the substituents on 3'-FP and 5-HF for P450s 1A1 and 1A2 are located in the sterically beneficial regions. The oxygen atoms of the side chains of these molecules are found in the red electrostatic region which favors negatively charged substituents, thereby contributing to their increased potencies. The contour maps from the QSAR analysis of the flavones for P450 enzymes 1A1 and 1A2 will help in the design of new derivatives with suitable substituents that can take advantage of the favorable steric and electrostatic effects.

In conclusion, a series of propargyl ether derivatives of hydroxy flavones and hydroxy flavanones were synthesized and assayed for their inhibition of P450 enzymes 1A1, 1A2, 2B1, and 2A6. Most of the compounds inhibited P450s 1A1 and 1A2 while none of them inhibited P450 2A6. Only two of the present compound series (2'-PF and 6-PFN) inhibited P450 2B1. Docking studies revealed that flavone propargyl ethers extended the reach of the ligands in the binding cavities for efficient oxidation, thereby increasing their potency. QSAR analysis of the series of compounds of the present study coupled with other flavone derivatives from our earlier studies yielded good QSAR models for P450 enzymes 1A1 and

1A2. These computational studies can help in the design of new derivatives that can potentially increase the potency and probably the selectivity of the inhibitors.

Acknowledgments

NIH-MBRS SCORE (grant number S06 GM 08008) for support of the preliminary work done on this project by the Foroozesh research group.

Louisiana Cancer Research Consortium for purchase of software licenses, NIH-RCMI (grant number G12RR026260) for support of the Molecular Structure and Modeling Core, and NIH-SCORE (grant number SC1GM084722) for research support for CLS and salary support for JS.

ABBREVIATIONS

P450	cytochrome P450
PAHs	polycyclic aromatic hydrocarbons
QSAR	quantitative structure activity relationship
EROD	7-ethoxyresorufin O-deethylation
MROD	7-methoxyresorufin O-demethylation
PROD	7-pentoxyresorufin O-depentylation
MOE	Molecular Operating Environment
MOPAC	Molecular Orbital Package
SD	steepest descent
SG	conjugate gradient
TN	truncated Newton
rms	root mean square
CoMFA	Comparative Molecular Field Analysis
CPSA	Charged Partial Surface Area

REFERENCES

1. Kuhnau J. The flavonoids. A class of semi-essential food components: their role in human nutrition. *World Rev. Nutr. Diet.* 1976; 24:117–91. [PubMed: 790781]
2. Arct J, Pytkowska K. Flavonoids as components of biologically active cosmeceuticals. *Clin. Dermatol.* 2008; 26:347–57. [PubMed: 18691514]
3. Kale A, Gawande S, Kotwal S. Cancer phytotherapeutics: role for flavonoids at the cellular level. *Phytother. Res.* 2008; 22:567–77. [PubMed: 18398903]
4. Zhang S, Yang X, Coburn RA, Morris ME. Structure activity relationships and quantitative structure activity relationships for the flavonoid-mediated inhibition of breast cancer resistance protein. *Biochem. Pharmacol.* 2005; 70:627–39. [PubMed: 15979586]
5. Moridani MY, Pourahmad J, Bui H, Siraki A, O'Brien PJ. Dietary flavonoid iron complexes as cytoprotective superoxide radical scavengers. *Free Radic. Biol. Med.* 2003; 34:243–53. [PubMed: 12521606]
6. Inoue T, Sugimoto Y, Masuda H, Kamei C. Antiallergic effect of flavonoid glycosides obtained from *Mentha piperita* L. *Biol. Pharm. Bull.* 2002; 25:256–9. [PubMed: 11853178]

7. Bear WL, Teel RW. Effects of citrus flavonoids on the mutagenicity of heterocyclic amines and on cytochrome P450 1A2 activity. *Anticancer Res.* 2000; 20:3609–14. [PubMed: 11131669]
8. Hodek P, Trefil P, Stiborova M. Flavonoids-potent and versatile biologically active compounds interacting with cytochromes P450. *Chem. Biol. Interact.* 2002; 139:1–21. [PubMed: 11803026]
9. Shimada T, Tanaka K, Takenaka S, Murayama N, Martin MV, Foroozesh MK, Yamazaki H, Guengerich FP, Komori M. Structure-Function Relationships of Inhibition of Human Cytochromes P450 1A1, 1A2, 1B1, 2C9, and 3A4 by 33 Flavonoid Derivatives. *Chem. Res. Toxicol.* 2010; 23:1921–1935. [PubMed: 21053930]
10. Kim HJ, Lee SB, Park SK, Kim HM, Park YI, Dong MS. Effects of hydroxyl group numbers on the B-ring of 5,7-dihydroxyflavones on the differential inhibition of human CYP 1A and CYP1B1 enzymes. *Arch. Pharm. Res.* 2005; 28:1114–21. [PubMed: 16276964]
11. Tsujimoto M, Horie M, Honda H, Takara K, Nishiguchi K. The structure-activity correlation on the inhibitory effects of flavonoids on cytochrome P450 3A activity. *Biol. Pharm. Bull.* 2009; 32:671–6. [PubMed: 19336903]
12. Walle T. Methoxylated flavones, a superior cancer chemopreventive flavonoid subclass? *Semin. Cancer Biol.* 2007; 17:354–62. [PubMed: 17574860]
13. Zhu N, Lightsey D, Foroozesh M, Alworth W, Chaudhary A, Willett KL, Stevens CK. Naphthoflavone propargyl ether inhibitors of cytochrome P450. *J. Chem. Crystallogr.* 2006; 36:289–296.
14. Gobbi S, Cavalli A, Rampa A, Belluti F, Piazza L, Paluszczak A, Hartmann RW, Recanatini M, Bisi A. Lead optimization providing a series of flavone derivatives as potent nonsteroidal inhibitors of the cytochrome P450 aromatase enzyme. *J. Med. Chem.* 2006; 49:4777–80. [PubMed: 16854084]
15. Lu YF, Santostefano M, Cunningham BD, Threadgill MD, Safe S. Substituted flavones as aryl hydrocarbon (Ah) receptor agonists and antagonists. *Biochem. Pharmacol.* 1996; 51:1077–87. [PubMed: 8866830]
16. Kimura Y, Ito H, Ohnishi R, Hatano T. Inhibitory effects of polyphenols on human cytochrome P450 3A4 and 2C9 activity. *Food Chem. Toxicol.* 2010; 48:429–35. [PubMed: 19883715]
17. Otake Y, Walle T. Oxidation of the flavonoids galangin and kaempferide by human liver microsomes and CYP1A1, CYP1A2, and CYP2C9. *Drug Metab. Dispos.* 2002; 30:103–5. [PubMed: 11792676]
18. Roberts DW, Doerge DR, Churchwell MI, Gamboa da Costa G, Marques MM, Tolleson WH. Inhibition of extrahepatic human cytochromes P450 1A1 and 1B1 by metabolism of isoflavones found in *Trifolium pratense* (red clover). *J. Agric. Food Chem.* 2004; 52:6623–32. [PubMed: 15479032]
19. Si D, Wang Y, Zhou YH, Guo Y, Wang J, Zhou H, Li ZS, Fawcett JP. Mechanism of CYP2C9 inhibition by flavones and flavonols. *Drug Metab. Dispos.* 2009; 37:629–34. [PubMed: 19074529]
20. Walle UK, Walle T. Bioavailable flavonoids: cytochrome P450-mediated metabolism of methoxyflavones. *Drug Metab. Dispos.* 2007; 35:1985–9. [PubMed: 17709371]
21. Quintieri L, Palatini P, Nassi A, Ruzza P, Floreani M. Flavonoids diosmetin and luteolin inhibit midazolam metabolism by human liver microsomes and recombinant CYP 3A4 and CYP3A5 enzymes. *Biochem. Pharmacol.* 2008; 75:1426–37. [PubMed: 18191104]
22. Zhai S, Dai R, Friedman FK, Vestal RE. Comparative inhibition of human cytochromes P450 1A1 and 1A2 by flavonoids. *Drug Metab. Dispos.* 1998; 26:989–92. [PubMed: 9763404]
23. Zhai S, Dai R, Wei X, Friedman FK, Vestal RE. Inhibition of methoxyresorufin demethylase activity by flavonoids in human liver microsomes. *Life Sci.* 1998; 63:PL119–23. [PubMed: 9718089]
24. Ortiz de Montellano PR. Mechanism-based inactivation of cytochrome P450: isolation and characterization of N-alkyl heme adducts. *Methods Enzymol.* 1991; 206:533–40. [PubMed: 1784239]
25. Ortiz de Montellano PR, Komives EA. Branchpoint for heme alkylation and metabolite formation in the oxidation of arylacetylenes by cytochrome P-450. *J. Biol. Chem.* 1985; 260:3330–6. [PubMed: 3972828]
26. Ortiz de Montellano PR, Kunze KL. Self-catalyzed inactivation of hepatic cytochrome P-450 by ethynyl substrates. *J. Biol. Chem.* 1980; 255:5578–85. [PubMed: 7380828]

27. Halpert J. Further studies of the suicide inactivation of purified rat liver cytochrome P-450 by chloramphenicol. *Mol. Pharmacol.* 1982; 21:166–72. [PubMed: 7132955]
28. Halpert J, Neal RA. Inactivation of purified rat liver cytochrome P-450 by chloramphenicol. *Mol. Pharmacol.* 1980; 17:427–31. [PubMed: 7393219]
29. Davies HW, Britt SG, Pohl LR. Inactivation of cytochrome P-450 by 2-isopropyl-4-pentenamide and other xenobiotics leads to heme-derived protein adducts. *Chem. Biol. Interact.* 1986; 58:345–52. [PubMed: 3742647]
30. Davies HW, Britt SG, Pohl LR. Carbon tetrachloride and 2-isopropyl-4-pentenamide-induced inactivation of cytochrome P-450 leads to heme-derived protein adducts. *Arch. Biochem. Biophys.* 1986; 244:387–92. [PubMed: 3947068]
31. Davies HW, Satoh H, Schulick RD, Pohl LR. Immuno-chemical identification of an irreversibly bound heme-derived adduct to cytochrome P-450 following CCl₄ treatment of rats. *Biochem. Pharmacol.* 1985; 34:3203–6. [PubMed: 4038333]
32. Foroozesh M, Primrose G, Guo Z, Bell LC, Alworth WL, Guengerich FP. Aryl acetylenes as mechanism-based inhibitors of cytochrome P450-dependent monooxygenase enzymes. *Chem. Res. Toxicol.* 1997; 10:91–102. [PubMed: 9074808]
33. Hopkins NE, Foroozesh MK, Alworth WL. Suicide inhibitors of cytochrome P450 1A1 and P450 2B1. *Biochem. Pharmacol.* 1992; 44:787–96. [PubMed: 1510726]
34. Roberts ES, Hopkins NE, Foroozesh M, Alworth WL, Halpert JR, Hollenberg PF. Inactivation of cytochrome P450s 2B1, 2B4, 2B6, and 2B11 by arylalkynes. *Drug Metab. Dispos.* 1997; 25:1242–8. [PubMed: 9351899]
35. Sridar C, Kent UM, Noon K, McCall A, Alworth B, Foroozesh M, Hollenberg PF. Differential inhibition of cytochromes P450 3A4 and 3A5 by the newly synthesized coumarin derivatives 7-coumarin propargyl ether and 7-(4-trifluoromethyl)coumarin propargyl ether. *Drug Metab. Dispos.* 2008; 36:2234–43. [PubMed: 18653744]
36. Strobel SM, Szklarz GD, He Y, Foroozesh M, Alworth WL, Roberts ES, Hollenberg PF, Halpert JR. Identification of selective mechanism-based inactivators of cytochromes P-450 2B4 and 2B5, and determination of the molecular basis for differential susceptibility. *J. Pharmacol. Exp. Ther.* 1999; 290:445–51. [PubMed: 10381811]
37. Zhu N, Lightsey D, Liu J, Foroozesh M, Morgan KM, Stevens ED, Klein Stevens CL. Ethynyl and Propynylpyrene Inhibitors of Cytochrome P450. *J. Chem. Crystallogr.* 2010; 40:343–352. [PubMed: 20473363]
38. Chan WK, Sui Z, Ortiz de Montellano PR. Determinants of protein modification versus heme alkylation: inactivation of cytochrome P450 1A1 by 1-ethynylpyrene and phenylacetylene. *Chem. Res. Toxicol.* 1993; 6:38–45. [PubMed: 8448348]
39. Roberts ES, Hopkins NE, Alworth WL, Hollenberg PF. Mechanism-based inactivation of cytochrome P450 2B1 by 2-ethynyl-naphthalene: identification of an active-site peptide. *Chem. Res. Toxicol.* 1993; 6:470–9. [PubMed: 8374044]
40. Kagawa H, Takahashi T, Ohta S, Harigaya Y. Oxidation and rearrangements of flavanones by mammalian cytochrome P450. *Xenobiotica.* 2004; 34:797–810. [PubMed: 15742975]
41. Burke MD, Thompson S, Weaver RJ, Wolf CR, Mayer RT. Cytochrome P450 specificities of alkoxyresorufin O-dealkylation in human and rat liver. *Biochem. Pharmacol.* 1994; 48:923–36. [PubMed: 8093105]
42. Buters JT, Schiller CD, Chou RC. A highly sensitive tool for the assay of cytochrome P450 enzyme activity in rat, dog and man. Direct fluorescence monitoring of the deethylation of 7-ethoxy-4-trifluoromethylcoumarin. *Biochem. Pharmacol.* 1993; 46:1577–84. [PubMed: 8240414]
43. DeLuca JG, Dysart GR, Rasnick D, Bradley MO. A direct, highly sensitive assay for cytochrome P-450 catalyzed O-deethylation using a novel coumarin analog. *Biochem. Pharmacol.* 1988; 37:1731–9. [PubMed: 3259881]
44. Sridhar J, Jin P, Liu J, Foroozesh M, Stevens CL. In silico studies of polyaromatic hydrocarbon inhibitors of cytochrome P450 enzymes 1A1, 1A2, 2A6, and 2B1. *Chem. Res. Toxicol.* 2010; 23:600–7. [PubMed: 20078084]

45. Oda A, Yamaotsu N, Hirono S. New AMBER force field parameters of heme iron for cytochrome P450s determined by quantum chemical calculations of simplified models. *J. Comput. Chem.* 2005; 26:818–26. [PubMed: 15812779]
46. Gill, PE.; Murray, W.; Wright, MH. *Practical Optimization*. Academic Press. London: p. 1981
47. McKendall M, Smith T, Ahn K, Ellis J, McGee T, Foroozesh M, Zhu N, Stevens CK. Methoxyflavone Inhibitors of Cytochrome P450. *J. Chem. Crstallogr.* 2008; 38:231–237.
48. Sridhar J, Liu J, Foroozesh M, Stevens CL. Insights on cytochrome p450 enzymes and inhibitors obtained through QSAR studies. *Molecules.* 2012; 17:9283–305. [PubMed: 22864238]

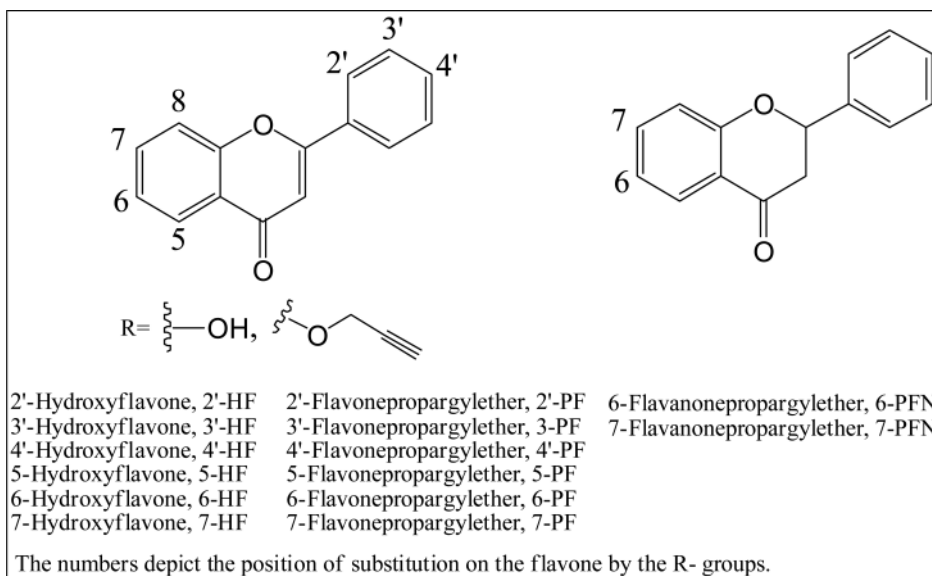


Fig. (1).
Structures of hydroxy flavones, flavone propargyl ethers, and flavanone propargyl ethers.

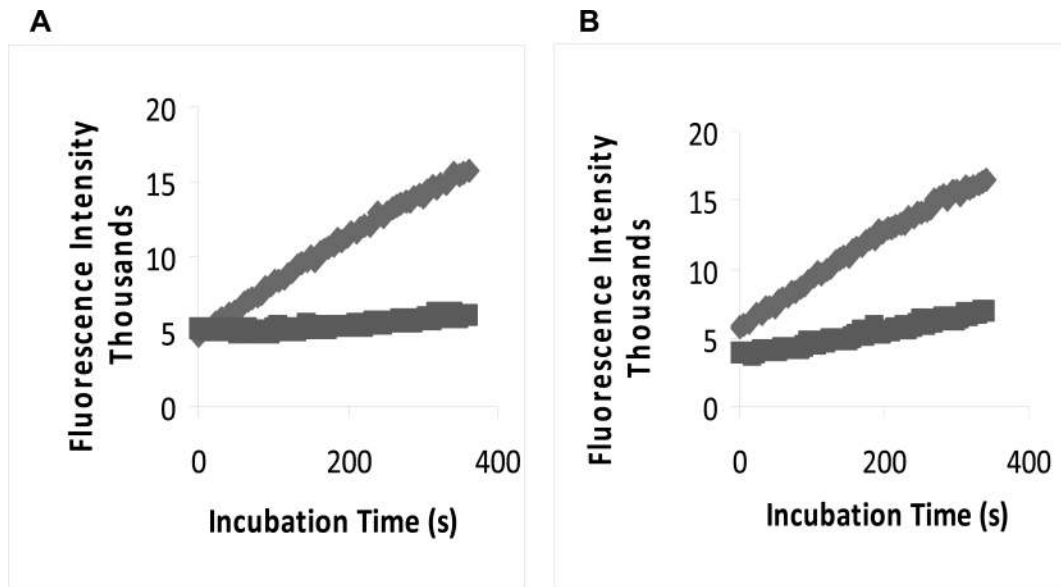


Fig. (2). Resorufin anion formation by P4501A1-dependent EROD in the presence of 0.016 μM 3'-PF(A) and 5 μM 7-HF (B) after 5 minute pre-incubation in the presence (■) or absence (◆) of NADPH.

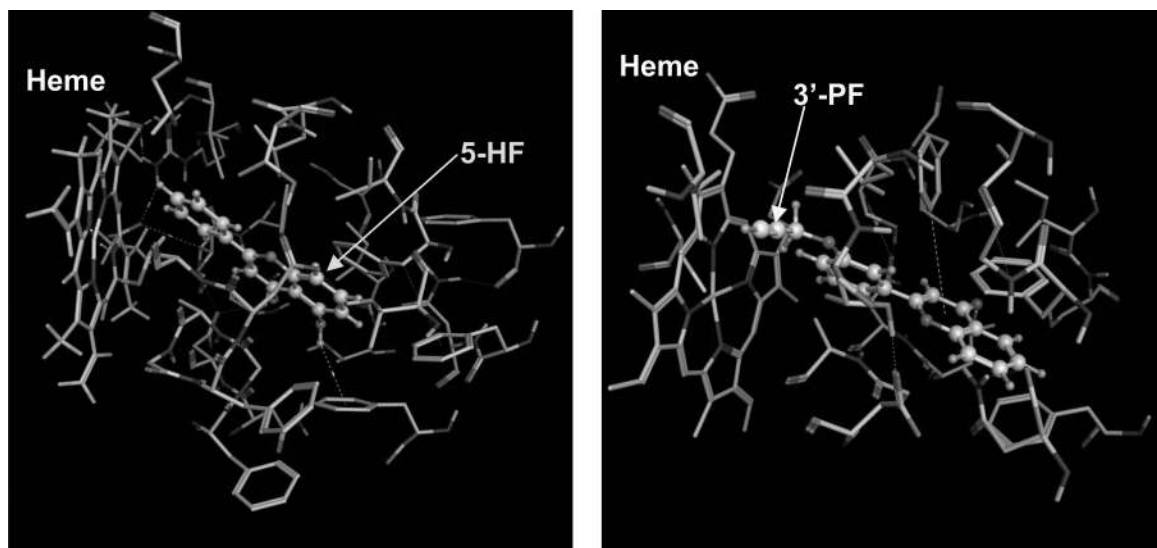


Fig. (3). Binding modes of 5-hydroxy flavone to P450 1A2 (**A**) and 3'-flavone propargyl ether to P450 1A1 (**B**). The protein residues are shown as stick models and the ligands are shown as ball and stick models.

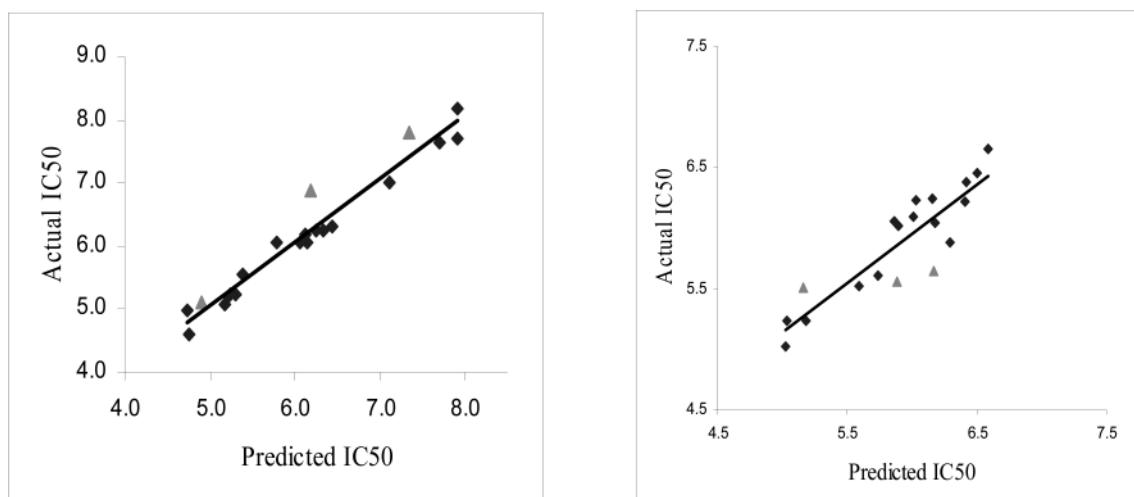


Fig. (4). Relationship between the actual and predicted log IC₅₀ values for the P450 1A1 (A) and 1A2 (B) models. Data points representing the test compounds that were not included in the training set of the QSAR analysis are colored red.

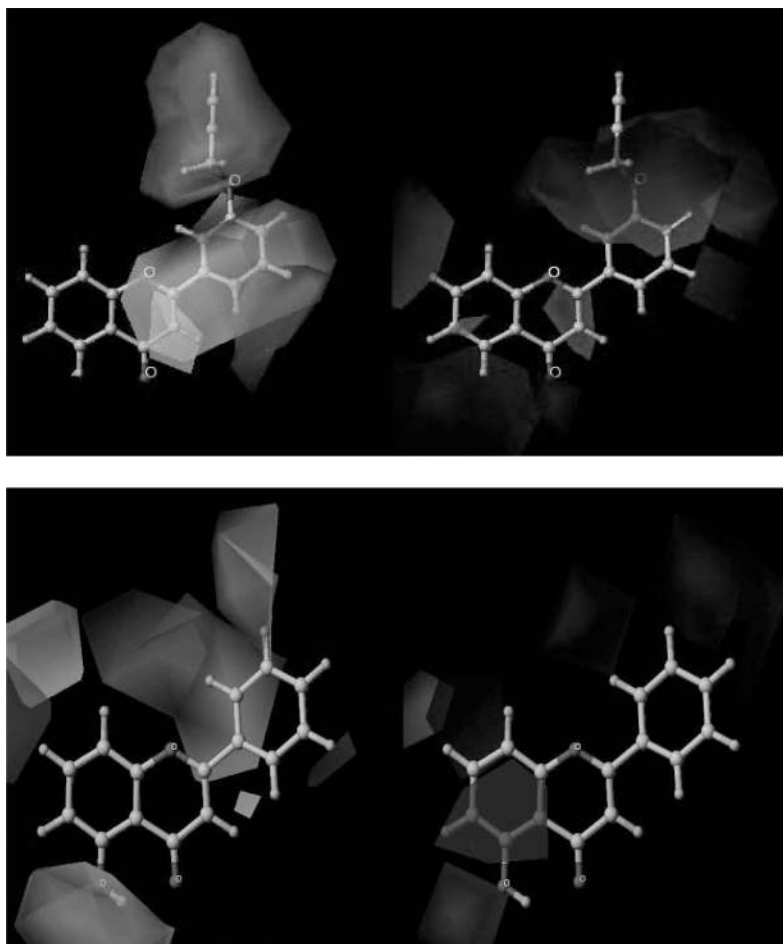


Fig. (5). CoMFA contour maps for the most active compound 3'-PF against P450 1A1 (A) and most active compound 5-HF against P450 1A2. Steric desirable and undesirable contours are colored green and yellow; +ve charge and -ve charge desirable contours are colored blue and red.

Table 1

Inhibition of P450 Enzymes 1A1, 1A2, 2B1 and 2A6 by Hydroxy Flavones, Flavone Propargyl Ethers, and Flavanone Propargyl Ethers

Compound	IC ₅₀ (μ M)			
	1A1	1A2	2B1	2A6
2'-HF	17.71	9.39	>50	>50
3'-HF	5.00	9.22	>50	>50
4'-HF	18.29	6.52	>50	>50
5-HF	4.03	0.31	>50	>50
6-HF	12.36	6.92	>50	>50
7-HF	6.79	2.55	>50	>50
2'-PF	0.56	1.29	9.66	>10
3'-PF	0.02	0.67	>10	>10
4'-PF	0.65	1.27	>10	>10
5-PF	1.60	0.38	>10	>10
6-PF	0.48	0.71	>10	>10
7-PF	0.51	0.41	>10	>10
6-PFN	5.77	>10	2.35	>10
7-PFN	5.98	0.97	>10	>10

Table 2

Mechanism-based Inhibition of P450 1A1 by 3'-Flavone Propargyl Ether (3'-PF) and 7-Hydroxy Flavone (7-HF)

Compound	$K_i(\mu\text{M})$	Limit $k_{inact}(\text{min}^{-1})$
3'-PF	0.24	0.090
7-HF	2.43	0.115

Table 3

Actual (EL) and Predicted (PL) logIC₅₀ (9-logIC₅₀) Values Together from CoMFA Analyses for the Inhibitors of P450 1A1 (A) and 1A2 (B)

A			B		
Compound	EL	PL	Compound	EL	PL
2'-αPNF	7.1192	7.0183	2'-αPNF	5.8601	6.0617
2'-βPNF	7.9208	7.7183	2'-βPNF	6.2924	5.8869
2'-PF	6.2518	6.2465	2'-HF	5.0273	5.0225
2'-HF	4.7518	4.5921	3FM	5.7328	5.6066
3',4'-DFM	6.0555	6.0528	3'-PF	6.1739	6.0439
3'-FM	6.1249	6.1871	3'-HF	5.0353	5.2333
3'-PF	7.6990	7.6314	4'-αPNF	6.585	6.6589
3'-HF	5.3010	5.2277	4'-βPNF	6.1549	6.2488
4'-FM	6.1487	6.0566	4'-PF	5.8962	6.0134
4'-αPNF	7.9208	8.1683	4'-HF	5.1858	5.2325
4'-HF	4.7378	4.9858	5-PF	6.4202	6.3801
5-PF	5.7959	6.0622	5-HF	6.5086	6.4503
5-HF	5.3947	5.5598	6-PF	6.0269	6.2259
6-PFN	5.2388	5.2499	7-PFN	6.0132	6.0965
6-PF	6.4318	6.3014	7-PF	6.4089	6.2152
7-PFN	5.2233	5.2028	7-HF	5.5935	5.5174
7-PF	6.3279	6.2436	2'-PF*	5.8894	5.5588
7-HF	5.1681	5.0636	4'-FM*	6.1675	5.651
4'-βPNF*	7.3468	7.8020	6-HF*	5.1599	5.5093
4'-PF*	6.1871	6.8746			
6-HF*	4.9080	5.1074			

* Compounds that were not included in the training set of the 3D-QSAR model.